J|A|C|S
COMMUNICATIONS

Published on Web 02/12/2008

Plasmon-Based Nanolenses Assembled on a Well-Defined DNA Template

Sébastien Bidault,*,† F. Javier García de Abajo,‡ and Albert Polman†

Center for Nanophotonics, FOM Institute AMOLF, Kruislaan 407, 1098 SJ Amsterdam, The Netherlands, and Instituto de Óptica, CSIC, Serrano 121, 28006 Madrid, Spain

Received December 18, 2007; E-mail: sebastien.bidault@normalesup.org

The high local fields exhibited by noble-metal nanostructures excited at their plasmon resonance make them strong candidates for molecular sensing with an optical readout in the visible to near-infrared range. For instance, surface enhanced Raman scattering (SERS) provides spectroscopic information on probe molecules placed in electromagnetic hot spots with up to single-molecule sensitivity (SM-SERS).[1] However, SM-SERS is typically observed for molecules aggregated by chance between closely spaced particles where the field is highest.[1] As a step toward SM-SERS by design, we demonstrate here the synthesis of well-defined groupings of 5, 8, and 18 nm diameter Au particles with nanometer spacings (Figure 1b−d). These structures are readily obtained by hybridizing monoconjugated DNA−particle building blocks (see Figure 1a). Generalized Mie theory calculations show that these particle groupings feature intensity enhancements that reach 4 orders of magnitude and provide guidelines to further optimize these local fields.

Theoretical studies have demonstrated that particle aggregates only exhibit high-enough local fields to justify SM-SERS when spacings reach a few nanometers,[2] introducing the concept of coupled metal particles as nanolenses.[2b] Such a distance is beyond the resolution of typical top-down fabrication procedures like e-beam and optical lithographies or focused ion-beam milling. Numerous studies have recently been devoted to novel bottom-up,[3a−c] electrochemical,[3d,e] or optical[3f] techniques for the fabrication of coupled plasmonic nanostructures as SERS active substrates. One particularly promising procedure is the assembly of noble-metal nanoparticles on DNA scaffolds. DNA molecules can be programmed to self-assemble into complex 2D and 3D objects.[4] Furthermore, gold nanoparticles can be readily linked to a controlled number of thiolated DNA molecules, allowing the synthesis of discrete 5 or 10 nm diameter gold particle groupings.[5] Using more complex DNA scaffolds, extended[6a,b] or dynamic[6c] particle assemblies were recently demonstrated.

Most published DNA templated gold nanostructures feature interparticle distances of tens of nanometers.[5,6a,b] In order to bring particle spacings down to the nanometer range, we functionalize one gold nanoparticle with a 5′ thiolated DNA molecule and the other with the 3′ thiolated complementary strand (see Figure 1a). Following published procedures,[5] we use electrophoresis to isolate phosphine-coated 5, 8, and 18 nm diameter particles functionalized with a known number of thiolated DNA single strands (see Supporting Information (SI) for further details). 8 nm Au particles linked to one single 100-base single-stranded DNA molecule (100b ss-DNA) yield building blocks **1** (see Figure 1a). More complex building blocks can be synthesized by sequential monofunctionalization with DNA strands of different sequences and lengths such as **2** with two 50b and 100b ss-DNA molecules. DNA hybridization drives the assembly of **3**, **4**, and **5,** which are then imaged by electron microscopy (EM, Figure 1b−d). These asymmetric geometries are chosen not only to study the influence of relative particle sizes and curvatures but also to ensure the obtained groupings did not result from random aggregation. Analysis of the EM images allows us to estimate final sample purities of 75%, 60%, and 50% for **3**, **4**, and **5**, respectively (see SI). In practice, 70% of groupings **3** (Figure 1b) exhibit particle spacings below 1 nm with similar values for **4** and **5**.

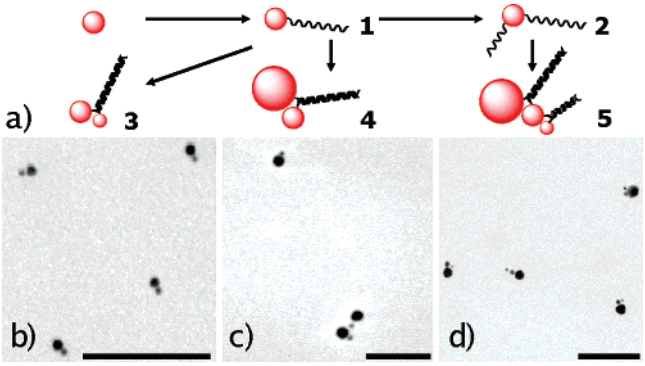

Figure 1. (a) Nanoparticle assembly scheme. 8 nm diameter Au particles are attached to one 5′ thiolated 100b ss-DNA molecule to produce building blocks **1**. **1** is sequentially functionalized with a 5′ thiolated 50b ss-DNA molecule to yield **2**. Hybridization of **1** with 5 and 18 nm diameter Au particles monofunctionalized with the 3′ thiolated complementary strand yields structures **3** and **4**. **5** is obtained by hybridizing **3** with 5 and 18 nm particles monofunctionalized with the 3′ thiolated 50b and 100b complementary strands, respectively. EM images of **3** (b, TEM), **4** (c, SEM), and **5** (d, TEM). Bar is 100 nm.

We use generalized Mie theory (GMT) to model plasmon mode coupling in groupings **3**, **4**, and **5**. This method is based on the spherical vector wave expansion of electric and magnetic fields in each particle reference frame followed by a translation in the aggregate coordinate system.[7] It allows for an analytical description of the multiple scattering processes occurring in sphere aggregates excited by an incoming plane wave. For computational reasons, the spherical expansion must be limited to maximum multipolar and scattering orders for which convergence is verified. Figure 2a shows the maximum intensity enhancement (I^{enh}), compared to the incoming field, estimated for groupings **3** and **4** with particle spacings ranging from 0.5 to 5 nm ($n = 1.5$ refractive index environment). The gold dielectric constant is taken from published experimental data[8] and corrected for the particle size, as it is comparable to the electron mean free path in Au[9] (see SI). I^{enh} is estimated at the resonance for the longitudinal plasmon mode, where the enhanced fields are highest. Resonance frequencies are derived from the scattering cross section of the particle grouping with an incoming polarization parallel to the dimer. At spacings smaller than 1 nm, I^{enh} typically reaches 3 orders of magnitude and up to 4 orders in **4**. The maximum field is always found at the surface of the smaller particle since it features the highest curvature. Comparing 0.5 and 5 nm spacings, I^{enh} drops by nearly 2 orders of magnitude, demonstrating the need for interparticle distance minimization as offered by our synthetic scheme. Stronger enhance-

† FOM Institute AMOLF.
‡ Instituto de Óptica.

10.1021/ja711074n CCC: $40.75 © 2008 American Chemical Society

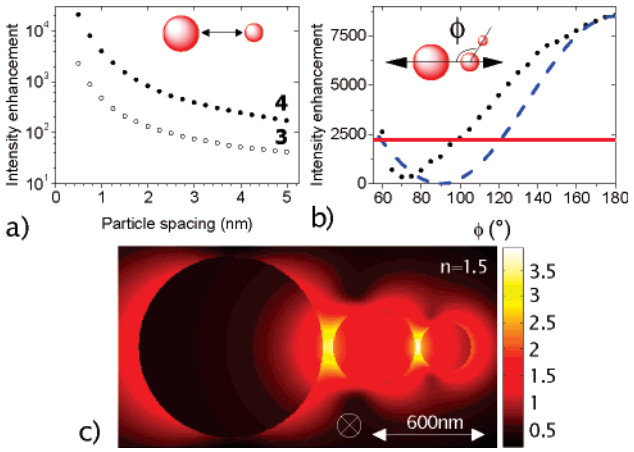

Figure 2. (a) Calculated maximum intensity enhancement (I^{enh}) in the gap of groupings **3** (○) and **4** (●) for particle spacings ranging from 0.5 to 5 nm ($n = 1.5$ dielectric environment). (b) Evolution of I^{enh} on the surface of the 5 nm particle in groupings **5** (1 and 0.5 nm spacings), for ϕ ranging from 60° to 180° and incoming polarization along the 8−18 nm particles axis. The red line corresponds to I^{enh} in grouping **3** for 0.5 nm spacing, and the dashed blue line is a $\cos^2(\phi)$ evolution. (c) I^{enh} (logarithmic scale) in aligned 18, 8, and 5 nm spheres with 1 and 0.5 nm spacings, respectively. 25 multipoles and 30 orders of scattering are used for the calculation with convergence verified for **4** with 0.5 nm spacing and **5** with 1 and 0.5 nm spacings.

ment factors in **4** as compared to **3**, at constant spacings, are due to increasing particle polarizability for larger spheres. I^{enh} for **3** and **4** are nearly identical if plotted versus spacing/diameter, as this is a good parameter of the plasmon coupling strength in particle dimers.[10] Furthermore, in dimers, I^{enh} increases with particle size at a constant spacing up to sphere diameters of 60 nm after which radiation damping brings the enhancement down (see SI). In our experimental conditions, suspensions of phosphine-coated gold particles can only be monofunctionalized with DNA for diameters lower than 20 nm.

By combining spheres of decreasing diameters in grouping **5**, it is possible to couple longitudinal plasmon modes and progressively increase the particle curvature.[2b] To keep the plasmon coupling similar between consecutive spheres, we consider 1 and 0.5 nm spacings between the 18−8 nm and 8−5 nm particles, respectively (Figure 2b and c). Comparing an aligned grouping **5** to groupings **3** and **4** with identical spacings, we find that I^{enh} is similar between the larger particles but is increased by a factor of 4 on the surface of the 5 nm sphere (Figure 2c). The plasmon mode interaction is dependent on the angle ϕ defined by the three particles. Figure 2b shows the evolution of I^{enh} on the 5 nm particle for ϕ ranging from 60° to 180° (typically observed on EM images) while keeping the incoming polarization parallel to the 8−18 nm particle axis. While I^{enh} between the 8 and 18 nm particles is essentially independent of ϕ, it varies over a factor of 30 on the 5 nm particle in this angle range. The evolution of I^{enh} deviates substantially from a $\cos^2(\phi)$ variation that would be expected for a dipolar plasmon interaction (blue dashed line in Figure 2b). This demonstrates the influence of higher multipolar modes at subnanometer interparticle spacings. Figure 2c also shows that I^{enh} is significantly larger in **5** than in a single 8−5 nm dimer (red line in Figure 2-b) for ϕ larger than 120°, which corresponds to about 30% of **5** according to EM images. For ϕ smaller than 65°, the spacing between the 5 and 18 nm particles drops below 1 nm, explaining the increase of I^{enh}. Calculations performed on **5** with larger particle spacings exhibit similar evolutions of I^{enh} with ϕ. **5** thus features similar or larger enhancement factors than the equivalent dimers **3** and **4** combined. However, field optimization in **5** requires a rigid DNA template[4a,b] where angle and spacings can be engineered.

In conclusion, we present a simple and reproducible method to assemble gold nanoparticles on DNA templates with high purities, nanometer spacings, and control over relative particle size. Mie calculations predict field intensities enhanced by 4 orders of magnitude in groupings **4** and **5**, which should permit SERS measurements using novel interferometric techniques adapted to particles smaller than 20 nm.[11] These nanostructures should, therefore, feature high local fields in proximity to a well-defined biomolecular backbone that can be further modified and functionalized. Our calculations also pinpoint which parameters should be tuned to optimize I^{enh}. In practice, larger passivated gold particles[12] on rigid DNA templates[4a,b] should allow for plasmonic sensors with single-molecule sensitivity.

Acknowledgment. We thank S. A. Claridge, R. N. Zuckermann, and A. P. Alivisatos for stimulating discussions. H. Meeldijk is gratefully acknowledged for the TEM measurements and A. F. Koenderink for his input on GMT calculations. Part of this work was performed at the Molecular Foundry, Lawrence Berkeley National Laboratory, which is supported by the Office of Science, Office of Basic Energy Sciences, of the U.S. Department of Energy under Contract No. DE-AC02−05CH11231. This work is part of the research program of FOM and was partially supported by NANONED.

Supporting Information Available: Experimental protocols, EM images, particle size influence. This material is available free of charge via the Internet at http://pubs.acs.org.

References

(1) (a) Kneipp, K.; Wang, Y.; Kneipp, H.; Perelman, L. T.; Itzkan, I.; Dasari, R.; Feld, M. S. *Phys. Rev. Lett.* **1997**, *78*, 1667−1670. (b) Nie, S. M.; Emory, S. R. *Science* **1997**, *275*, 1102−1106.

(2) (a) Xu, H. X.; Aizpurua, J.; Kall, M.; Apell, P. *Phys. Rev. E* **2000**, *62*, 4318−4324. (b) Li, K. R.; Stockman, M. I.; Bergman, D. J. *Phys. Rev. Lett.* **2003**, *91*, 227402.

(3) (a) Wei, A.; Kim, B.; Stadtler, B.; Tripp, S. L. *Chem. Phys. Chem.* **2001**, *12*, 743−745. (b) Wang, H.; Levin, C. S.; Halas, N. J. *J. Am. Chem. Soc.* **2005**, *127*, 14992−14993. (c) Ringler, M.; Klar, T. A.; Schwemer, A.; Susha, A. S.; Stehr, J.; Raschke, G.; Funk, S.; Borowski, M.; Nichtl, A.; Kurzinger, K.; Phillips, R. T.; Feldmann, J. *Nano Lett.* **2007**, *7*, 2753−2757. (d) Qin, L. D.; Zou, S. L.; Xue, C.; Atkinson, A.; Schatz, G. C.; Mirkin, C. A. *P. Natl. Acad. Sci. U.S.A.* **2006**, *103*, 13300−13303. (e) Ward, D. R.; Grady, N. K.; Levin, C. S.; Halas, N. J.; Wu, Y. P.; Nordlander, P.; Natelson, D. *Nano Lett.* **2007**, *7*, 1396−1400. (f) Svedberg, F.; Li, Z. P.; Xu, H. X.; Kall, M. *Nano Lett.* **2006**, *6*, 2639−2641.

(4) (a) Winfree, E.; Liu, F. R.; Wenzler, L. A.; Seeman, N. C. *Nature* **1998**, *394*, 539−544. (b) Rothemund, P. W. K. *Nature* **2006**, *440*, 297−302. (c) Shih, W. M.; Quispe, J. D.; Joyce, G. F. *Nature* **2004**, *427*, 618−621. (d) Aldaye, F. A.; Sleiman, H. F. *J. Am. Chem. Soc.* **2007**, 13376−13377.

(5) Zanchet, D.; Micheel, C. M.; Parak, W. J.; Gerion, D.; Williams, S. C.; Alivisatos, A. P. *J. Phys. Chem. B* **2002**, *106*, 11758−11763.

(6) Examples of 1D and 2D Au arrays: (a) Deng, Z. X.; Tian, Y.; Lee, S. H.; Ribbe, A. E.; Mao, C. D. *Angew. Chem., Int. Ed.* **2005**, *44*, 3582−3585. (b) Zheng, J. W.; Constantinou, P. E.; Micheel, C.; Alivisatos, A. P.; Kiehl, R. A.; Seeman, N. C. *Nano Lett.* **2006**, *6*, 1502−1504. (c) Aldaye, F. A.; Sleiman, H. F. *J. Am. Chem. Soc.* **2007**, *129*, 4130−4131.

(7) García de Abajo, F. J. *Phys. Rev. Lett.* **1999**, *82*, 2776−2779.

(8) Johnson, P. B.; Christy, R. W. *Phys. Rev. B* **1972**, *6*, 4370−4379.

(9) (a) Hövel, H.; Fritz, S.; Hilger, A.; Kreibig, U.; Vollmer, M. *Phys. Rev. B* **1993**, *48*, 18178−18188. (b) Stoller, P.; Jacobsen, V.; Sandoghdar, V. *Opt. Lett.* **2006**, *31*, 2474−2476.

(10) Jain, P. K.; Huang, W.; El-Sayed, M. A. *Nano Lett.* **2007**, *7*, 2854−2858.

(11) Lindfors, K.; Kalkbrenner, T.; Stoller, P.; Sandoghdar, V. *Phys. Rev. Lett.* **2004**, *93*, 037401.

(12) Reinhard, B. M.; Sheikholeslami, S.; Mastroianni, A.; Alivisatos, A. P.; Liphardt, J. *Proc. Natl. Acad. Sci. U.S.A.* **2007**, *104*, 2667−2672.

JA711074N